Thermochimica Acta, 65 (1983) 359–374
Elsevier Science Publishers B.V., Amsterdam – Printed in The Netherlands

THERMAL AND SPECTROSCOPIC INVESTIGATIONS OF SOME EGYPTIAN CLAYS

EGLAL R. SOUAYA, SUZY A. SELIM and SAMI K. TOBIA

Department of Chemistry, Faculty of Science, Ain Shams University, Abbassia, Cairo (Egypt)

(Received 3 January 1983)

ABSTRACT

Nine clay specimens taken from various sites in Egypt and belonging to different epochs have been examined by TG, DTA, IR and XRD for their characterisation.

A method is proposed using essentially TG data, by which it was possible to differentiate between kaolinitic and non-kaolinitic clays.

The content of some trace elements, namely, iron, potassium and manganese, in the clays can be used to identify kaolins. No correlation could be observed between the epoch of deposition and the nature of the clay mineral content.

INTRODUCTION

The vast industrial applications of clays makes their identification a must. This identification includes not only the constituent clay minerals but also the trace impurities [1]. Archaeologists have tried to correlate the pattern of the trace impurities in ancient pottery with that found in the clays which were probably used for their manufacture [2,3].

Modern methods of chemical analysis such as emission spectroscopy [4,5] and neutron activation analysis [6] have been used. A study between the epoch of deposition and the trace impurities of some selected Egyptian clays have been reported [2,7] without reference to their clay mineral constitution.

Clays are usually analysed by the use of techniques such as X-ray fluorescence [8] and X-ray diffraction [9–12] in which case it is difficult to identify poorly crystallised kaolins. Infrared spectroscopy is however becoming an important tool for such qualitative identification [13,14]. Thermal studies of clay minerals using TG and DTA were mainly confined to the monitoring of the dehydration processes [9a,15–17] or to the effect of cation additions on the thermal effects produced [9a], but scarcely any identification of the constituent clay minerals [18–20] was achieved using TG analysis.

The location of the hydroxyl group in the lattice of the clay mineral is undoubtedly related to its structure and consequently to the amount of sorbed water. Though the presence of different cations of varying hydration

0040-6031/83/$03.00

capacities may bear some contribution to this sorbed water, it is relatively very small and could be neglected. In the present investigation, a method is introduced for distinguishing between kaolinitic and non-kaolinitic clays using the dehydration and dehydroxylation steps produced from TG analysis data. This identification, coupled with IR and DTA analyses is further confirmed by XRD patterns.

Samples of Egyptian clays belonging to different epochs and previously analysed by neutron activation for their trace element content [2] are studied in this investigation, in an attempt to reveal any relation between the trace element patterns and the nature of the clay minerals constituting the clay.

EXPERIMENTAL

Nine specimens, taken from different sites throughout Egypt and belonging to different epochs, are studied in this investigation. These are listed according to their geographical locations.

(a) Samples from south Egypt constituting those from (i) Kalabsha (cretaceous); (ii) shaft near Aswan taken at various depths (lower cretaceous) namely top layer, near top layer and at 75 m depth; (iii) Qena (recent) and (iv) Esna (Pleistocene).

(b) Samples from central Egypt taken from (i) Tora (Pleistocene) being situated near Cairo city and (ii) Wadi Abu-Agag (recent) situated near the Suez Gulf.

(c) A sample from Baharia Oasis (Pliocene clay) being situated in north centre of West Egypt.

Heating is achieved at 900°C for all samples except otherwise mentioned.

In the text the samples are grouped according to their thermal dehydration curves obtained by thermogravimetric analysis which actually constituted the same group of clay minerals. TG analysis was carried out in static air using a Stanton Redcroft thermobalance type 750/770, the heating rate being 10°C min^{-1}.

In the differential thermal analysis, α-alumina was used as inert standard and a program temperature controller, "Ether" transitrol type 994/2, was used to permit a linear rate of heating, i.e. 10°C min^{-1}. A Cambridge Recorder Model "B" was used for recording the temperature difference.

X-Ray diffraction patterns were obtained by means of a General Electric X-ray diffraction unit, Model XRD-6, using Ni-filtered Cu radiation. The *d* distances were calculated and compared with their relative intensities in the ASTM cards [21,22].

RESULTS AND DISCUSSION

Samples from Kalabsha and Wadi Abu-Agag

Thermogravimetric analysis curves of these two samples bear great similarity to one another: both show a small initial water loss below 100°C which is physically adsorbed and not exceeding ~1% followed by a limited gradual loss up to ~500°C [Fig. 1(A)]. Above this temperature, a rapid loss of lattice water (hydroxyls) takes place which terminates at ~ 800°C for the

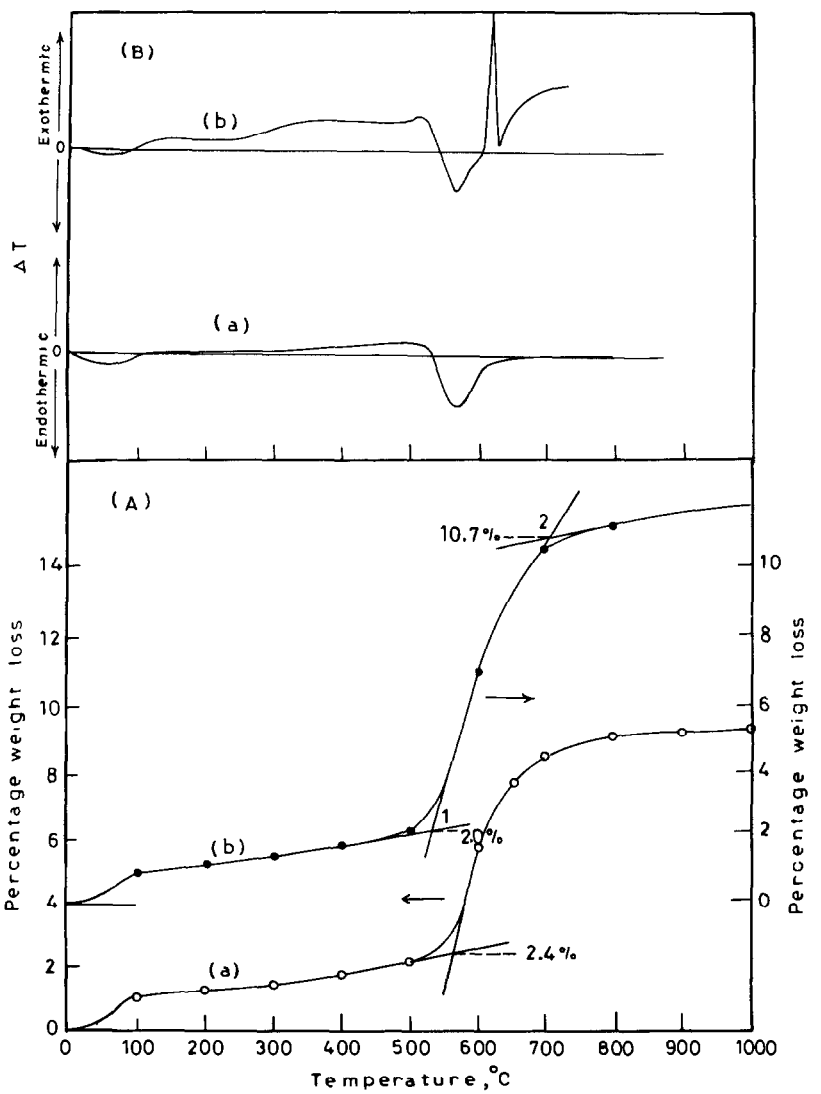

Fig. 1. TG and DTA curves for samples from (A) Wadi Abu-Agag and (B) Kalabsha zones.

TABLE 1

Some characteristic weight changes obtained from TG analysis data

Sample (zone)	Total loss (%)	Loss < 200°C (%)	Apparent loss of hydroxyls (%)	W_a
Wadi Abu-Agag	9.1	1.0	6.7	6.7
Kalabsha	11.6	0.8	7.8	9.7
Aswan top layer	11.6	2.0	2.9	1.5
Aswan near top	12.7	2.5	2.1	0.9
Aswan 75m deep	20.4	4.9	4.5	0.9
Baharia	22.5	2.9	3.0	1.0
Tora	18.6	6.8	7.1	1.0
Qena	16.5	7.6	5.5	0.7
Esna	12.0	4.2	3.8	0.9

sample from Wadi Abu-Agag. The Kalabsha sample shows an extended gradual loss in the range 700–1000°C. The total weight loss obtained by heating up to 1000°C is given in Table 1, column 2.

From the general shape of the TG curve and the values of the various decomposition steps, it is possible to predict the predominant clay mineral component and whether it is a kaolin or non-kaolin, e.g. mica. Water in kaolinites exists as hydroxyl groups such that they may be characterized by loss of very little or a negligible amount of adsorbed water at low temperatures, but above the range 400–500°C, the evolution of hydroxyl lattice water commences giving rise to one single step which may terminate at temperatures reaching 800°C. If the value of this step, taken from TG curves as percentage loss, is divided by that below 200°C, which represents physically adsorbed water, a numerical value is obtained for the amount of lattice water (hydroxyls) associated with unit weight of adsorbed water denoted for convenience by the symbol W_a. From a survey on clay mierals [9] it has been found that the amount of physically adsorbed water (< 200°C) is an important function of the nature of the clay mineral. For kaolinites to be present in a significant amount, the value for W_a must exceed at least 5. Whereas for montmorillonites or illites, for example, it is below ~2.00. As the kaolinite content in the clay decreases, the value of W_a decreases below 5. The value of 5 is taken as an arbitrary average as found from the samples in this investigation as well as others done in this laboratory. Both samples from Wadi Abu-Agag and Kalabsha give a value of W_a above 5 as shown in Table 1 showing them to be predominantly composed of kaolinites. The presence of a wide range of values above 5 results from the presence of a fraction of a non-decomposable non-clay fraction, e.g. quartz or of a small non-kaolinite fraction.

For the Kalabsha sample, the small extension of water loss up to 1000°C

results from its contamination with another clay mineral. In such a case a fraction of the hydroxyl decomposition in the range 500–800°C belongs to a clay mineral other than kaolinite. Assuming that the decompositions commencing at high temperatures (e.g. above 700°C) is proportional to the non-kaolinite fraction, its value is then subtracted from the actual decomposition step in the range 500–600°C before evaluating W_a as most micas lose lattice hydroxyls in this range as well. Thus, for the Kalabsha sample this is done by taking actual values of the decomposition steps from the intercepts (1) and (2) shown in Fig. 1(A). Thus, subtracting (1) from (2), e.g. 10.7–2.0% gives 8.7% from which is subtracted 0.9% [11.6 (total) – 10.7%] to give a value of 7.8 for the percentage loss considered to belong to the kaolinite fraction in the range 500–600°C. As the values so obtained may not necessarily result from kaolinites, as in cases where W_a is < 2.0, this percentage loss will be referred to as "apparent loss of hydroxyls" (Table 1, column 4).

IR spectra of these two samples are similar, where the location of the O–H vibrational frequencies, and therefore its attachment to either the Al^{3+}

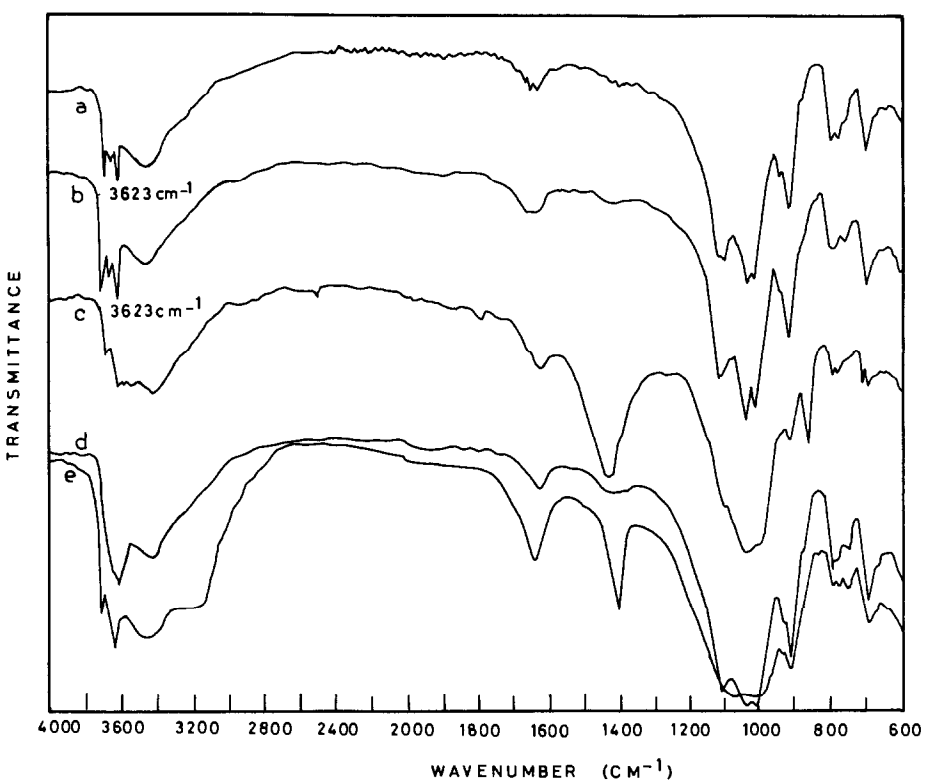

Fig. 2. Infrared spectra for samples from (a) Wadi Abu-Agag, (b) Kalabsha, (c) 75 m depth-Aswan, (d) Top-layer Aswan, (c) Tora.

octahedrals or Si^{4+} tetrahedrals are comparable and similar to those characterising kaolinites [23,24] (see Fig. 2, curves a and b). The O–H stretching frequencies are observed at 3623, 3650 and 3700–3705 cm^{-1}. The band at 3623 cm^{-1} is assigned to hydroxyl groups located inside the sheet, being situated at the middle layer between the tetrahedrals and octahedrals which form the kaolinite. The other bands at 3650 and 3700–3710 cm^{-1} are assigned to those hydroxyl groups constituting one side of the sheet, sometimes referred to as inner-surface hydroxyls [24]. For a well-crystallized kaolinite an additional band at 3670 cm^{-1} should also appear, which also constitutes an inner-surface hydroxyl [24]. Its absence in the present clays shows that our kaolinite is poorly crystalline.

The presence of two distinct IR absorption bands at 3623 and 3700 cm^{-1} of comparable intensities and having between them one or two smaller bands, according to the sample crystallinity, confirms the presence of kaolinite as the predominant constituent, especially when XRD patterns fail to identify the poorly crystalline forms.

It is also of significance that the presence of the strongest band of the hydroxyl series at 3623 cm^{-1} indicates the presence of a kaolinite structure. In non-kaolinite clay minerals, it is shifted to 3630–3635 cm^{-1} (see, for example, Fig. 2, curves c and d).

The results obtained from TG and IR analyses are confirmed by X-ray analysis data. The clear band at 7.17 Å and those at 2.566, 3.579 and 4.366 Å which are destroyed by heating at 500°C are characteristic of kaolinites [22a] and those at 3.34, 4.26 and 1.82 Å are characteristic of α-quartz [21a]: these bands form the main constituents. The existence of a broad band in the 2θ range of 7.0–9.5 Å for the Kalabsha sample points to

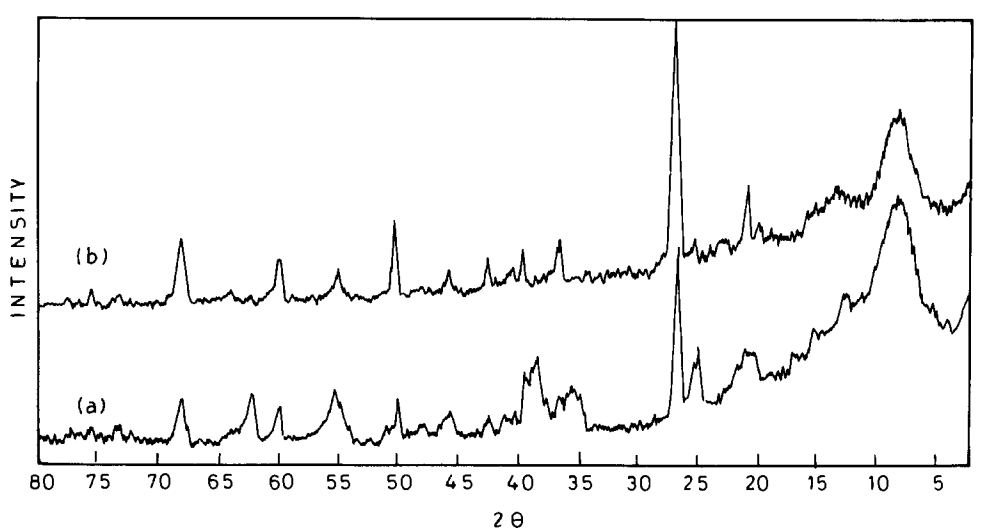

Fig. 3. XRD patterns for (a) unheated and (b) heated samples from Kalabsha.

the existence of some mica (Fig. 3). The absence of attalpugite is confirmed by the absence of zeolitic water [9a]. The XRD patterns of the heated products of these two samples are also identical.

The DTA curves exhibit a very small endotherm at ~100°C and a strong one at 570°C [Fig. 1(B)] which reproduce the effects observed from the TG analysis. However, for the Kalabsha sample, a shoulder is observed at ~600°C which is immediately followed by a sharp exotherm at 620°C. No structural phases could be identified from X-ray analysis of both heated and unheated samples, that would explain this exothermic effect, except that the bands characteristic of α-quartz are intensified. As the shoulder at 600°C results from the dehydration of the quartz present [9b] it is plausible to attribute this exotherm to the cystallisation of some non-crystalline quartz present in the specimen, which takes place immediately after this dehydration process. All the phase transformations of quartz are known to be endothermic in nature [15].

Analysis of these samples by the neutron activation technique [2] has revealed that they are characterised by low iron (~0.7–~1.2% as oxide), low potassium (0.1–0.2% as oxide) and low manganese (up to 0.07% as oxide) contents. These low percentages seem characteristic for kaolins as has also been found with other samples [2].

Specimens from a shaft near Aswan, at different depths and Baharia Oasis

The thermogravimetric analysis curve of the sample taken at 75 m depth shows great similarity to that from Baharia Oasis though both belong to different epochs. Those from top and near top layers are different but bear some similarity to each other [Fig. 4(A)]. All samples exhibit three main distinct steps: (i) below 200°C, (ii) in the temperature range 500–650°C and preceded by a gradual increase starting at 300°C, and (iii) in the temperature range 650–850°C for samples of top and near top layers and 750–950°C for the other two samples. Though the decomposition step in the temperature range 500–650°C arises from the dehydroxylation of the clay, that at higher temperatures for the Baharia and 75 m depth samples could not possibly result from a dehydroxylation process alone.

From an examination of the IR spectra of these samples (Fig. 2c), the absence of kaolinite or even a clay of kaolinitic structure is at once conceived. The band of maximum intensity characterising the O–H vibration is observed at 3630 cm^{-1} and that at 3710 cm^{-1} is of least intensity showing the presence of a mica structure. A large broad band at 1440 cm^{-1} is observed for the 75 m depth sample and Baharia samples only, which points to the presence of a large fraction of a carbonate [25] probably calcite, whose presence is responsible for the large decomposition step in the high temperature range [26].

For the evaluation of W_a for these two samples it is reasonable to exclude

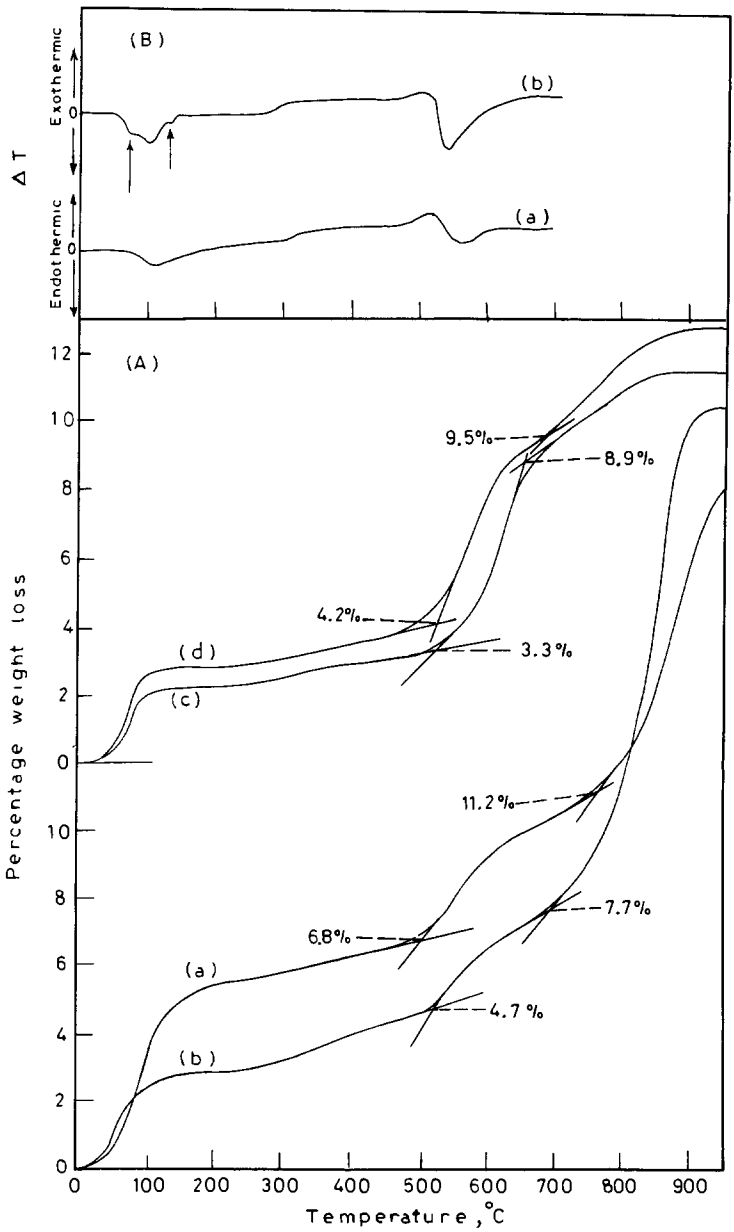

Fig. 4. (A) TG curves for samples from (a) 75 m depth-Aswan clay, (b) Baharia oasis, (c) top-layer Aswan clay, (d) near top-layer Aswan clay. (B) DTA curves for samples from Aswan (a) 75 m depth and (b) top layer.

the last decomposition step resulting from a non-clay fraction. Accordingly, values of ~0.9 and ~1.0 are obtained for the 75 m depth and Baharia samples, respectively.

With regard to the Aswan samples taken at top and near top layers, W_a is

evaluated in the same way as for the Kalabsha sample. All W_a values are far below 5 (Table 1, column 5) showing, together with the IR spectra of the hydroxyl vibrations, the complete absence of kaolinite or any clay with a kaolinite structure.

The XRD patterns of these samples confirm this identification. The presence of well-defined peaks at d distances of 3.06, 3.309 and 1.885 Å for the 75 m depth and the Baharia sample, point to the presence of a large fraction of calcite [21b], which is converted to the oxide [21c] in their heated products (Fig. 5). The presence of α-quartz for these two samples is also identified in their XRD patterns.

A broad band is observed for all samples at 2θ range below 12° which points to the presence of a hydromica. The appearance of some small peaks in the 2θ range of 5.0–8.8°, which are more pronounced for the Baharia sample, show the presence of a clay of the montmorillonite group [27]: these peaks are shifted to higher 2θ values upon heating to 300°C. The various small peaks appearing in this region result from the high contamination of the montmorillonite clay. The incorporation of several cations of small sizes

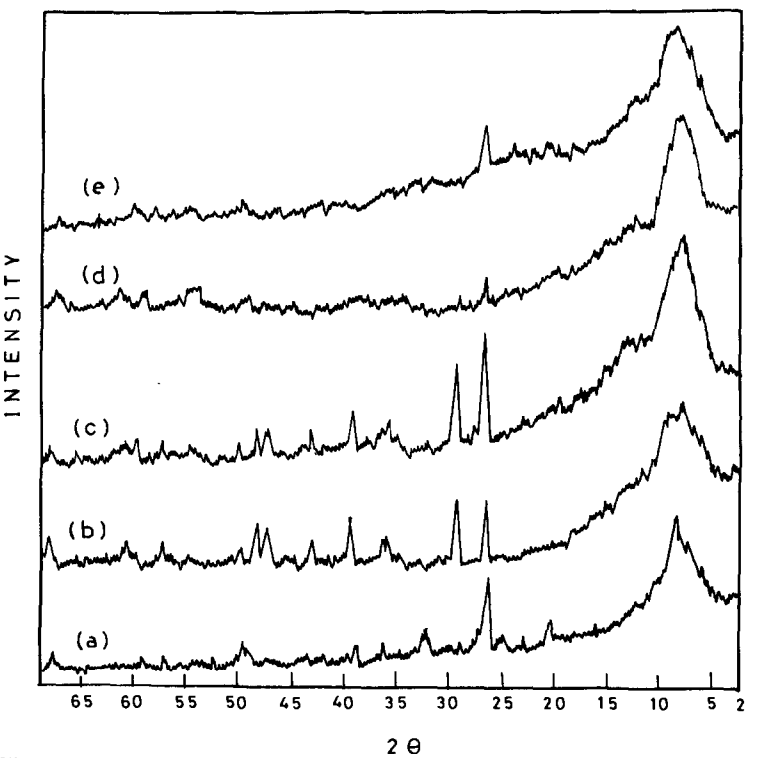

Fig. 5. XRD patterns for (a) heated and (b) unheated samples from Baharia oasis; (c) unheated sample at 75 m depth from Aswan clay; (d) unheated and (e) heated samples from top layer.

into the octahedral lattice structure or their replacement by some of the aluminium ions produce various dislocations. The presence of some chloride, probably chamosite, of chlorite-type structure, is not to be ignored as the band at a *d* distance of ~7.2 Å is not affected by heating and the band at ~14.7 Å is intensified. A montmorillonite–chlorite appears to be present [22b].

The bands observed at *d* distances of 10.08 and 3.365 Å characterize the presence of illite which appears to be muscovite of the 1 Md polytype [28]. These bands are unaffected by heating.

The DTA curves up to 650°C reproduce the similarity observed in the corresponding TG curves [Fig. 4(B)]. Two main endothermic effects are observed centered at ~100°C with a shoulder at ~130°C, being characteristic of dehydration, and at 545°C which is responsible for the dehydroxylation process. For samples from top and near top layers, the first endotherm is preceded by a shoulder at ~60°C which probably results from water which is attached to some already adsorbed water layers, thus requiring little energy for its detachment. The presence of the endotherm at 100°C and the shoulder at 130°C point to the desorption of water which is directly attached to the solid surface and which indicates the presence of two different energy sites on the solid. It is of significance to mention here that in some montmorillonites the first endotherm at ~(120–130°C) is accompanied by a shoulder at ~200°C [15] depending on the hydration energies of the different cations. In the present situation, the main endotherm occurs at ~100°C which is not characteristic of montmorillonites. Moreover, the small differences observed in the concentration of the cations present in the various samples [2], could not possibly give rise to such a distinct shoulder at ~130°C. The only plausible interpretation would be the presence of two clay minerals, which is confirmed by the XRD analysis. These details are not revealed in the TG curves.

No endothermic effects are observed at temperatures between 300 and 400°C where a weight loss is observed. The decomposition of a nitrate present in the clay would be responsible for such a weight loss and should decompose exothermally [29]. However, no distinct exotherm is necessarily observed by such small amounts of incorporated salts or complexes [30] but an appreciable shift towards the exothermic direction is observed in this temperature range. Infrared spectral analysis shows a small broad band in the vicinity of ~1400 cm^{-1} which is characteristic of the presence of nitrate ions [25] (see Fig. 2d). It appears unlikely that ammonium salts would be stable under the prevailing environmental conditions, as ammonia would be evolved when the pH of the medium was > 7.

It is important to note that prior to the endothermic effect at ~540°C, a small broad exotherm is noticed which also appeared in most samples. Though it is known to result from grain growth of the particles, its existence immediately before the dehydroxylation of the clay shows that a process of

rearrangement takes place by which the dehydroxylation is facilitated. This may be a migration of the hydroxyl ions from their point of attachment.

In spite of the deposition of these samples at different epochs, they are similar not only in the clay mineral constituents but also in their corresponding cerium content, which is relatively high (145–320 p.p.m.) but not as high as that encountered with kaolins (371–480 p.p.m.) [2].

Specimens from Qena, Esna and Tora Zones

Four steps are observed in the TG analysis curve of the Qena sample: an initial large loss of adsorbed water below 200°C followed by a gradual loss in the temperature range 300–550°C, a large dehydroxylation step in the temperature range 550–700°C and a small step at ~870°C [Fig. 6 (A)].

For the evaluation of W_a, the last step occurring at 870°C should be excluded since IR spectral analysis shows a band at ~1410 cm^{-1} which may result from either a carbonate, probably calcite, or nitrate salts. The decomposition of calcite takes place at about this temperature and its presence is further confirmed by XRD analysis. However, the presence of some nitrate salt as well is not to be ignored. Accordingly, a value of 0.7 for W_a is obtained which shows the absence of a kaolin. Indeed, such a high initial water uptake is usually associated with illites and to some extent with some montmorillonite–chlorites.

The weight loss observed in the temperature range 300–550°C probably arises from the chlorite present. If the cation associated with the chlorite is Fe^{3+} or Fe^{2+}, the amount present being 9.8% [7], the dehydration from the brucite layer takes place at 250 and 430°C, respectively [31]. It seems likely that both forms of iron are present whereby a gradual loss in weight results from the dehydration of the brucite layer.

The sharp weight loss observed in the range 550–700°C results from the loss of hydroxyls from the illite and the mica layer of the chlorite.

The DTA curve produced with a heating rate of 15°C min^{-1} gave rise to one single endotherm at ~140°C, whereas if the heating rate is decreased to 7°C min^{-1} two distinct endotherms are observed at ~80 and ~150°C, the latter being smaller [Fig. 6(B)]. These two steps are not distinguished in the TG curve. The presence of a large fraction of illite and therefore a large amount of adsorbed water, which is usually evolved at temperatures $\leqslant$ 100°C, would hinder the appearance of a second step in this temperature range. The endotherm observed at ~150°C would therefore result from the chlorite fraction being interlayered with water which may accompany very fine-grained chlorites [9c].

No clear thermal effects could be observed which would correspond to the weight loss in the temperature range 300–550°C. Though the dehydration process should give rise to an endotherm, the decomposition of the nitrate salts present or any agglomeration of the grains resulting from the dehydra-

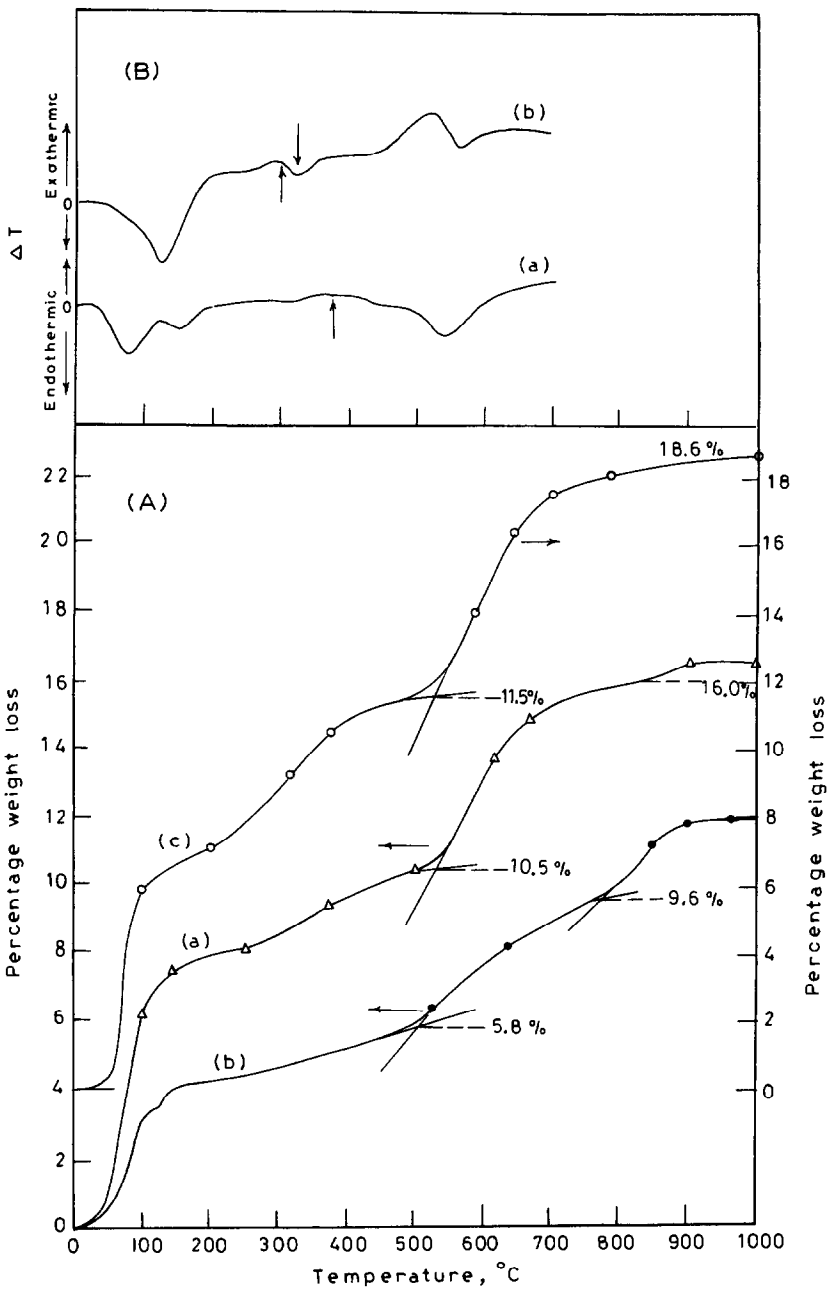

Fig. 6. (A) TG curves for samples from (a) Qena, (b) Esna and (c) Tora zones. (B) DTA curves for samples from (a) Qena and (b) Tora zones.

tion process, both would result in an exothermic effect. Compensation of these various thermal effects seem to hinder the appearance of each process separately, giving rise to a net small exothermic plateau covering the range 330–440°C. An endothermic peak is also observed at 540°C resulting from the dehydroxylation process.

The X-ray diffraction pattern of this sample shows this mixed-layer clay mineral to be predominantly composed of mica ($2M_1$) where the principal *d* spacing is at 10.4 Å (Fig. 7a). Consequently, illite [21d] forms the main constituent together with α-quartz, both of which are unaffected by heat. The presence of bands at *d* distances of 7.08 and 3.52 Å confirm the presence of a chlorite as those rich in iron give weak first and third basal reflections. Also, the absence of a band at 2.38 Å, which is a distinct third-order reflection for kaolinite, gives a strong confirmation of the identification [32]. Traces of montmorillonite may be present as well where, besides the XRD identification, a small band appears in the IR analysis at 915 cm^{-1}. The presence of calcite is deduced from the band at 3.035 Å in the XRD pattern: the calcite is converted to the oxide upon heating.

The thermogravimetric curve obtained for the Esna sample is similar to that from Qena with some variations in the relative amounts of each component [Fig. 6(b)]. At temperatures below 200°C, two steps are distinguished for the water adsorbed by illite and chlorite, respectively. The amount of adsorbed water which is associated with the illite fraction and evolved at ~100°C is much less than that for the Qena sample, showing the latter to contain more illite. The amount of calcite in the Esna sample is also larger than that in the Qena sample, as observed from the step at ~800–900°C, and the IR band at ~1435 cm^{-1}. No nitrate salts are present

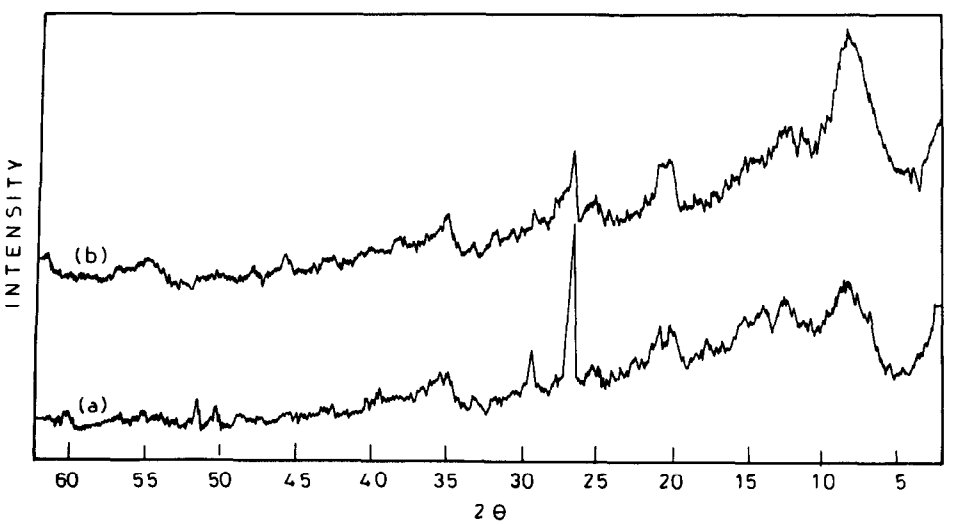

Fig. 7. XRD patterns for samples from (a) Qena and (b) Tora zones.

here and the intermediate weight loss in the temperature range 300–500°C is smaller and more gradual than that of the Qena sample. It arises only from the partial dehydration of the chlorite fraction. The evaluation of W_a, obtained by excluding the last step arising from the carbonate decomposition, gives a value of 0.9 (Table 1) showing the complete absence of a kaolin. The dehydroxylation of the clay is observed as a weight loss in the temperature range ~500–750°C.

The DTA of the Esna sample is similar to that of the Qena sample.

XRD patterns of this sample reproduce the foregoing conclusion besides showing the presence of some non-clay components, viz. ferriferous orthoclase and feldspar in minor amounts as observed from their corresponding relative intensities.

TG analysis of the sample from Tora shows three distinct steps covering the ranges 50–150, 200–500 and 500–900°C (Fig. 6c). The initial loss of adsorbed water is reproduced in the DTA curve by a large endotherm centered at ~130°C. That occurring in the range 200–500°C is accompanied by a small exotherm observed at 290°C followed by an endotherm at ~320°C. Infrared spectral analysis (Fig. 2e), shows a large band centered at ~3200 cm^{-1}, and a band at 1640 cm^{-1}, both being characteristic of the deformation vibration of water: these bands are larger than that observed for the previous samples. A band at ~3200 cm^{-1} was previously observed for water in zeolites [33]. The hydroxyl stretching vibration occurring at 3710 cm^{-1} is sharp and relatively intense resembling that for kaolinites but the presence of a band at 3635 cm^{-1} and not at 3623 cm^{-1} disproves its presence. Moreover, the value of W_a is ~1.0 which proves the absence of a kaolin. A plausible explanation would be the presence of a halloysite together with mica where the IR band at 915 cm^{-1} characterizes the presence of montmorillonites. The strong IR band at ~1400 cm^{-1} signifies the presence of a nitrate salt. The presence of any ammonium salts is ruled out by chemical analysis. Therefore, this step in the TG curve arises from both the dehydration of the halloysite and the thermal decomposition of the nitrate salt, the latter appearing as a small exotherm at ~290°C and the former as an endotherm at 320°C. The presence of these two consecutive processes at very close temperatures gives rise to the dual effect of subsiding each other resulting in very small energy changes [Fig. 6(B)].

The dehydroxylation step above 500°C is reproduced in the DTA curve at about 550°C and is preceded by a broad exotherm resulting from the grain growth of the particles.

X-Ray analysis of an unheated sample shows the presence of a randomly interstratified mixed layering of mica indicated by a series of reflections in the low angle side of about $2\theta = 8°$ [see Fig. 7(b)]. Identification of the pattern shows the predominant fractions to be illite [21d] and montmorillonite [22c] where the presence of different cations causes the appearance of several peaks in the broad band. The shift of the band to higher 2θ values

(~ 9 Å) observed upon heating characterises montmorillonite and confirms its presence. The pattern of halloysite is also observed which is destroyed upon thermal treatment.

Finally, it should be noted that no direct correlation could be traced between the present grouping of clays according to their TG analysis curves, and consequently, to their clay mineral constituents, and their trace element content as analyzed by neutron activation [2], except for very few cases where the iron, potassium and manganese contents may be used to differentiate between kaolinitic and non-kaolinitic clay minerals. Also, no correlation is observed between the epoch of deposition and the nature of the clay mineral content.

REFERENCES

1 K. Yamamoto, Bunseki, 10 (1979) 699.
2 S.K. Tobia and E.V. Sayre, in A. Bishay (Ed.), Recent Advances in Science and Technology of Materials, Vol. 3, Plenum, New York, 1974.
3 C. Mosser, Phys. Chem. Earth, 11 (1979) 315.
4 H.W. Catling, A.E. Stoyle and E.E. Richards, Ann. Br. School Athens, 58 (1963) 94.
5 A. Millett and H. Catling, Archaeometry, 9 (1966) 92.
6 V.M. Emeleus, Archaeometry, 1 (1958) 6. V.M. Emeleus and G. Simpson, Nature (London), 185 (1960) 196. G. Harbottle, Archaeometry, 12 (1970) 23. J.S. Clin and E.V. Sayre, in R.H. Brill (Ed.), Science and Archaeology, MIT Press, Cambridge, MA, 1971, Chap. 14.
7 S.K. Tobia, and E.R. Souaya, Egypt. J. Chem., 24 (1981) 131.
8 A. Podsiadly and J. Kolasinski, Szklo Ceram., 31 (1) (1980) 20.
9 R.E. Grim, Clay Mineralogy, McGraw Hill, New York, London, 1968, (a) p. 343; (b) p. 290; (c) p. 340.
10 P. Kamarchik, Jr., J. Coating Technol., 52 (666) (1980) 79.
11 F.H. Abdel Kader, M.L. Jackson and G.B. Lee, Soil Sci. Soc. Am. Proc., 42 (1) (1978) 163.
12 E. Abou Saif and E.J. Al Adl, Bull. NRC (Egypt), 2 (1977) 177.
13 M. Fieldes, R.J. Furkert and N. Wales, N.Z.J. Sci., 15 (4) (1972) 615.
14 J. Hlavay S. Elek and J. Inczedy, Hung. Sci. Instrum., 38 (1976) 69.
15 R.C. Mackenzie, (Ed.), Differential Thermal Analysis, Vol. 1, Academic Press, London, 1970.
16 G.B. Mangold, in L.W. Le Roy, D.O. Le Roy and J.W. Raese (Eds.), Subsurface Geology, Colorado School of Mines, 4th edn., (1977) 104.
17 R.C. MacKenzie, Thermochim. Acta, 28 (1979) 1.
18 J.P. Guha, Zambia J. Sci. Technol., 2 (2) (1977) 1.
19 R.G. Charles, Thermochim. Acta, 34 (1979) 309.
20 I.J. Smalley and G.S. Xidakis, Clay Sci., 5 (4) (1979) 189.
21 J.V. Smith, (Ed.) X-Ray Powder Data File and Index Data File, American Society for Testing and Materials, Philadelphia, 1961, (a) Card no. 5-0490; (b) card no. 5-0586; (c) card no. 4-0777; (d) card no. 9-343.
22 Powder Diffraction File, ASTM, Alphabetical Index of Inorganic Compounds, International Center for Diffraction Data, Pennsylvania, 1978, (a) Card no. 14-164; (b) card no. 7-51; (c) card no. 13-135.
23 R.L. Ledoux and J.L. White, Science, 47 (1964) 145; Clays Clay Miner., 13 (1964) 289.

24 P.G. Rouxhet, N. Samudacheeta, H. Jacobs and O. Anton, Clay Miner., 12 (1977) 171.
25 K. Nakamoto (Ed.), Infrared Spectra of Inorganic and Coordination Compounds, Wiley, New York, London, 1962.
26 C.D. Hodgman, (Ed.), Handbook of Chemistry and Physics, CRC Press, Cleveland, OH, 43rd edn., 1961.
27 D. Carroll, Clay Minerals. A Guide to their X-Ray Identification, The Geological Society of America, Boulder, CO, 1970.
28 H.S. Yoder and H.D. Eugster, Geochim. Cosmochim. Acta, 8 (5–6) (1955) 225.
29 W.W. Wendlant and I.P. Smith, J. Inorg. Nucl. Chem., 26 (1964) 445.
30 S.A. Selim, H.A. Hassan, M. Abd-El-Khalik and R.Sh. Mikhail, Thermochim. Acta, 45 (1981) 349.
31 S. Caillere and S. Henein, Bull. Soc. Fr. Ceram., 48 (1960) 63.
32 W.F. Bradley, X-Ray Diffraction Criteria of Chloritic Material, National Academy of Science, Publ. 327, 1954, pp. 324–334.
33 L. Bertsch and H.W. Habgood, J. Phys. Chem., 67 (1963) 1921.